

Investigation of Methane Hydrate Structure, Content and Source

Status Report

Reporting Period Start Date 10/01/01

Reporting Period End Date 12/31/02

Principal Author: Richard B. Coffin, Code 6115, EQSS, NRL, 4555 Overlook Ave., SW, Washington, DC, 20375

Report Issue Date December 23, 2002

DOE Award Number DE-AT26-97FT34344

Submitting Organization: Naval Research Laboratory, Code 6115, EQSS, 4555 Overlook Ave., SW, Washington, DC, 20375

Overview

Work in this report, funded by DOE/NETL, is separated into two projects. Dr. James Yesinowski is responsible for all activity in NMR analysis of the hydrates. Drs. Coffin and Grabowski are responsible for the carbon isotope analysis of the hydrates and sediments. Work described in the report includes field activity in the Gulf of Mexico and Cascadia Margin and laboratory experimentation.

Carbon Isotope Analysis of Methane Hydrates and Sediments

Dr. Richard B. Coffin, Code 6114
Dr. Kenneth S. Grabowski, Code 6371

1. Research Objective:

The objective of work reviewed through this report is to provide a natural system database to assist in understanding the biogeochemical influence on methane hydrate formation and content.

2. Introduction:

This work was conducted primarily on samples taken in the Cascadia Margin (CM) and Gulf of Mexico (GOM). In addition there is some comparison with data from samples taken in 1998 on the Haakon-Mosby Mud Volcano (HMMV) in the Norwegian-Greenland Sea. The HMMV is a cold seep off the coast of Norway with an active mud flow. Cascadia Margin is an accretionary prism of a subduction zone. The structure of this region has resulted in a recent tectonic compression and deformation. Hydrates in this region are found in silty clays and clayey silts interbedded with fine sand turbidites. The sample region in the Gulf of Mexico is a salt basin that formed from Late Triassic rifting of the Pangea super continent, and flooding by a thick salt deposit during middle Jurassic marine incursions. Thermogenic petroleum and gas deposits were produced from Miocene to Pleistocene reservoirs in the region. In this region over pressured fracture zones that surround moving salt diapirs and sheets provide active conduits for vertical migration from deep reservoirs to shallow pools and the surface. In this system hydrates are present in organic rich silty clays.

Sample analysis in this report employs radio and stable carbon isotopes to trace carbon cycling that influences the methane hydrate formation, stability and fate. Stable carbon isotope ratios vary as a function of the source of CO₂ that is transferred into organic matter through the autotrophic cycle, the enzymatic reaction in CO₂ fixation (Estep et al. 1978) and the rate that CO₂ is transferred into organic matter (Fogel et al. 1993). The $\delta^{13}\text{C}$ of contributing CO₂ sources have a broad range from approximately 0‰ to -50‰. A substantial source of oceanic CO₂ is atmospheric. The $\delta^{13}\text{C}$ of atmospheric CO₂ is approximately -7‰ depending on the region of the world. If atmospheric CO₂ is cycled by terrestrial plants there is an isotopic fractionation that occurs during the fixation that provides a range in $\delta^{13}\text{C}$ of approximately -30‰ to -12‰. The more depleted ¹³C value occurs in organisms that fix CO₂ via the Calvin-Benson cycle (Whelan et al., 1973), while relatively more ¹³C enrichment occurs with CO₂ fixation through the Hatch-Slack pathway (Estep et al. 1978). In the ocean CO₂ values are isotopically enriched to a range of -2‰ to 2‰ as a function of carbonate equilibrium. This results in enriched C¹³ isotope signatures in marine phytoplankton that range between -18‰ and -30‰ (Gearing et al., 1977; Sackett, 1991; Rau et al., 1989; 1991). In ocean sediment pore waters, active reduction of CO₂ results in a depleted ¹³C isotope signature. In regions of ocean sediment with active

biological methane cycling, the $\delta^{13}\text{C}$ of the CO_2 can be as isotopically depleted as -50‰ . This wide range in the $\delta^{13}\text{C}$ for CO_2 results in distinct isotope signatures between thermogenic and biogenic methane. Biogenic methane has been reported to be light in $\delta^{13}\text{C}$ with a range of -85‰ to -103‰ (Borowski et al., 1996; Borowski et al., 1997), with the lower value indicative of more active biogenic methane production. Thermogenic methane is substantially more enriched in ^{13}C with values in the range of -36‰ to -40‰ (Sassen and MacDonald, 1997).

With the complex cycling of carbon that is known in the ocean, additional tracers are required to determine the factors that contribute to methane hydrate production and stability. Radiocarbon is formed in the atmosphere when ^{14}N is altered by cosmic rays. The quantity of ^{14}C is a function of age, since upon isolation of a carbon pool, the half life of ^{14}C is 5370 years. As a result, $\Delta^{14}\text{C}$ of new organic matter recently produced in the ocean is elevated related to thermogenic carbon sources. In the ocean, $\Delta^{14}\text{C}$ ranges between approximately 100‰ and an undetectable value, near -1000‰ (Cherrier et al. 1999). There is a wide range of $\Delta^{14}\text{C}$ of dissolved organic carbon in the ocean that is related to the ocean circulation. Open ocean surface waters range between -150‰ to -258‰ (Williams and Druffel, 1987; Bauer et al. 1992, 1998; Druffel et al., 1992). Deeper ocean water, below 1000 m characteristically have $\Delta^{14}\text{C}$ that range from -393‰ to -525‰ (Williams and Druffel, 1987). A somewhat different range occurs for dissolved CO_2 , as reported in results of the World Ocean Circulation Experiment (WOCE) for the Pacific Ocean (von Reden et al 1997). In that work, the surface ocean waters have a $\Delta^{14}\text{C}$ range from about -50 to $+150\text{‰}$, while deeper waters below 1000 m have a range from about -160 to -220‰ .

3. Approach:

In the GOM cores were taken over locations that have active hydrate beds at the sediment water column interface. The Bush Hill and GC234 site coordinates are listed in Table 1. Sampling in the GOM was with push cores during submarine dives and surface sediment grabs. Typically 0.5-m cores were taken in the GOM and surface samples were obtained from these cores. Four different sites were sampled in the CM with a wide range in the hydrate abundance (Table 1). Cores were taken with a 10-m piston corer and ranged from 2 to 8-m. For the CM cores 10-20 sub-samples were obtained through the core profile. Cores C1 and C6 were taken at vent site with a region of blank seismic reflection which is believed to be vertical channels. Core C7 was taken at a site that was found to have a sharp scarp through previous seismic surveys. Cores from this location contained hydrates. Coring at C9 was in a region that a fishing boat recently pulled up a large load of surface hydrates in the net. Hydrates were not found in cores at region C9.

Table 1: Core sampling locations on the Texas-Louisiana Shelf in the Gulf of Mexico and Cascadia Margin along the coast of British Columbia, Canada.

| Station | Position | Water Depth (m) |
|-------------------------------|----------------------------|-----------------|
| Cascadia Margin C1 | 48°40.044'N, 126°50.751'W | 1267 |
| Cascadia Margin C6 | 48°39.966'N, 126°55.178'W | 1265 |
| Cascadia Margin C7 | 48°40.047'N, 126°51.067'W | 1264 |
| Cascadia Margin C9 | 48°40.099'N, 126°50.751'W | 840 |
| Gulf of Mexico Bush Hill (BH) | 27° 46.956'N, 91° 30.483'W | 550 |
| Gulf of Mexico GC234 | 27° 44.767'N, 91° 13.321'W | 570 |

4. Methods:

Work combines basic physical and chemical parameters analysis to investigate the sediment structure and content. The following methods were applied to the sample analyses.

a.) Stable Carbon Isotope ($\delta^{13}\text{C}$) Analysis

Stable carbon isotope analysis was conducted with samples in gas and solid phases. The $\delta^{13}\text{C}$ was measured with a Finnigan Delta S isotope ratio mass spectrometer (IRMS). Sediment samples were introduced to the IRMS with combustion in a Carlos Erba CNS 1000 instrument. Stable carbon isotope analysis for methane to hexane gases and carbonate is conducted with a gas phase inlet isotope ratio mass spectrometer. The gas chromatograph used was the Varian Star 3400 CX which is constructed to run samples (Varian, Harbor City, CA) in a parallel line with a Finnigan Magnum ion trap and a Finnigan Delta-S isotope ratio mass spectrometer (GC/ITMS/IRMS, Finnigan Corporation, San Jose, CA). The effluent from the column was split, 10% going to the ITMS for peak identification and the remainder to the IRMS where the analytes were combusted in line at 940 °C to CO_2 for isotope analysis. The two mass spectrometers provide peak identification simultaneous with the isotope analysis. The temperature profile through the GC runs started at 40°C and ramped to 180°C over 8 minutes. The $\delta^{13}\text{C}$ standard was Peedee Belminite. For the isotope ratio mass spectrometer, the detection limit is 1 $\mu\text{g C}$ and the precision is $\pm 0.3 \text{ ‰}$.

b.) Sediment Structure Analysis

Data presented here include sediment organic carbon content and grain size. Sediment grain size is broken into 3 phases with sand 2000 – 62 μm , silt 64 to 4 μm , and clay less than 4 μm (Ingram, 1971; Galehouse, 1971). At each core depth, 15-20 gm of sediment was sub-sampled from cores and treated with 30% H_2O_2 for 48-hr and subsequently washed with milli-Q water. Samples were then dispersed with 50 gm/l Calgon solution and wet sieved at 4 phi to separate sand and mud fractions. The mud fraction was then suspended in 1 L of DI water and samples were with drawn based on settling times

according to the Stoke's Law. Sand fraction was generally less than 5% of bulk weight for all samples. The settling time provided data at 4, 4.5, 5.5, 6, 7, 8, and 9 phi which corresponds to 64, 44, 31, 22, 16, 7.8, 3.9 and 1.95 μm , respectively. Vibration in the laboratory inhibited analysis of smaller particles.

Analysis of organic carbon content required volatilization of the inorganic carbon. This was accomplished by placing dried sediments in a bell jar with concentrated hydrochloric acid vapor on the jar base for 24 hours. After removal of the inorganic carbon, samples were dried a second time. Weighed sub-samples, approximately 5 mg, were run through the Carlo Erba sample introduction system for carbon isotope analysis and carbon content. All samples were run in triplicate.

c.) Organic Sediment $\delta^{13}\text{C}$

Sediments were treated as described for carbon content in section 4b and analyzed on the mass spec described in 4a. All samples were run in triplicate.

d.) Hydrate Content

The hydrate samples were placed in a 30 ml serum bottle and argon gas was streamed into the bottle to remove CO_2 in the air. Samples were sealed with aluminum and rubber septa. After the hydrates dissociated, 10-20 μl samples were taken with a 100 μl gas tight syringe from the bottles and injected into a GC. Samples were analyzed for methane, ethane, propane, butane, pentane and hexane concentrations. All samples were run in triplicate.

e.) Hydrate $\delta^{13}\text{C}$

For $\delta^{13}\text{C}$ of gases in the hydrates samples were prepared as described in section 4d. Gases were injected into the mass spectrometer described in section 4a. Gases that were analyzed included methane, ethane, propane, butane, pentane, hexane and carbon dioxide. All samples were run in triplicate.

f.) Bicarbonate $\delta^{13}\text{C}$

Dried sediment were placed in serum bottles and capped using the procedure described in section 4b. The samples were treated with 800 μl 85% phosphoric acid. The CO_2 in the serum bottle was removed with a gas tight syringe and injected in GC (section 4a) with the method described for methane analysis (section 4e). All samples were run in triplicate.

g) $\Delta^{14}\text{C}$ Analyses

Samples for radio carbon isotope analysis are prepared in a laboratory that is equipped with in line cryogenic distillation and graphitization hardware. Targets prepared in the NRL-Graphite Lab were analyzed at the NRL-TEAMS facility. This unique facility is

equipped with both a high intensity Cs sputter source used for ^{14}C analysis and a commercial secondary ion mass spectrometer (SIMS) used as an ion source for ultra-trace analysis. Its low and high energy transport systems allow simultaneous transport and analysis of a broad mass range ($M_{\text{max}}/M_{\text{min}} \sim 8$). Features of the system for ^{14}C analysis include a forty sample multi cathode ion source (model MC-SNICS) from National Electrostatics Corporation, a Pretzel recombinator magnet to simultaneously inject masses 12 to 14, a beam chopper to block mass 12 and 13 during measurement of ^{14}C , a 3 MV Pelletron tandem accelerator, an electrostatic 3° bend for charge state selection, a 30° electrostatic analyzer, and a split pole mass spectrograph for beam detection. Low noise Faraday cups and a solid state detector measure the relevant beam intensities. This system provides precise dating capabilities for ^{14}C analysis. This facility has been tested for background radio carbon and is capable of age dating to 50,500 years.

5. Results and Discussion

a). Sediment Properties

The data for sediment properties includes the organic carbon content analyzed on samples from the Cascadia Margin and Gulf of Mexico and grain size analysis on samples from the Cascadia Margin. The percent organic carbon in the Cascadia Margin cores from stations C1, C6 and C9 ranged between 0.390 and 0.738% (Table 2). There was not a large variation between these sites or through the individual cores. These values were lower than expected for the presence of hydrates. Future work will need to address the vertical methane migration relative to the microbial formation at the sample depth. The GOM samples are from two sites with large amounts of hydrates at the sediment-water column interface. At these sites the %C ranges from 1.25 to 17.07%. The high values are associated with regions of petroleum seeps through the ocean floor.

Table 2: Analysis of percent organic carbon in sediments from the Gulf of Mexico and Cascadia Margin.

| Core Site | Depth (cm) | % C | % C | % C | Average | s.d. |
|-----------------|------------|-------|-------|-------|---------|-------|
| Cascadia Margin | | | | | | |
| C9 | 5-10 | 0.500 | 0.500 | 0.483 | 0.494 | 0.010 |
| C9 | 15-20 | 0.611 | 0.592 | 0.583 | 0.595 | 0.014 |
| C9 | 25-30 | 0.537 | 0.525 | 0.547 | 0.536 | 0.011 |
| C9 | 35-40 | 0.481 | 0.470 | 0.456 | 0.469 | 0.013 |
| C9 | 45-50 | 0.359 | 0.343 | 0.360 | 0.354 | 0.010 |
| C9 | 75-85 | 0.609 | 0.583 | 0.546 | 0.579 | 0.032 |
| C9 | 105-115 | 0.490 | 0.478 | 0.493 | 0.487 | 0.008 |
| C9 | 145-155 | 0.594 | 0.574 | 0.580 | 0.583 | 0.010 |
| C9 | 295-300 | 0.387 | 0.401 | 0.395 | 0.394 | 0.007 |
| C9 | 300-310 | 0.420 | 0.415 | 0.449 | 0.428 | 0.018 |
| C9 | 405-420 | 0.435 | 0.437 | 0.445 | 0.439 | 0.005 |

| | | | | | | |
|----------------|---------|--------|--------|--------|--------|-------|
| C6 | 5-10 | 0.441 | 0.446 | 0.437 | 0.441 | 0.005 |
| C6 | 25-30 | 0.544 | 0.585 | 0.564 | 0.564 | 0.021 |
| C6 | 35-40 | 0.478 | 0.478 | 0.476 | 0.477 | 0.001 |
| C6 | 45-50 | 0.445 | 0.438 | 0.436 | 0.440 | 0.005 |
| C6 | 55-60 | 0.480 | 0.496 | 0.493 | 0.490 | 0.009 |
| C6 | 75-80 | 0.511 | 0.496 | 0.506 | 0.504 | 0.008 |
| C6 | 180-190 | 0.426 | 0.487 | - | 0.457 | 0.043 |
| C6 | 210-200 | 0.344 | 0.346 | 0.352 | 0.347 | 0.004 |
| C6 | 95-105 | 0.437 | 0.414 | 0.387 | 0.413 | 0.025 |
| C6 | 350-360 | 0.346 | 0.333 | - | 0.340 | 0.009 |
| C6 | 450-460 | 0.368 | 0.350 | - | 0.359 | 0.013 |
| C1 | 0-10 | 0.736 | 0.725 | 0.754 | 0.738 | 0.015 |
| C1 | 20-30 | 0.369 | 0.367 | 0.367 | 0.368 | 0.001 |
| C1 | 30-40 | 0.412 | 0.416 | 0.410 | 0.413 | 0.003 |
| C1 | 40-50 | 0.376 | 0.382 | 0.381 | 0.380 | 0.003 |
| Gulf of Mexico | | | | | | |
| BH | Surface | 3.099 | 2.990 | 3.150 | 3.080 | 0.082 |
| BH | Surface | 5.140 | 5.200 | - | 5.170 | 0.042 |
| BH | Surface | 9.160 | 9.640 | - | 9.400 | 0.339 |
| BH | Surface | 3.850 | 3.550 | 3.560 | 3.653 | 0.170 |
| BH | Surface | 1.230 | 1.280 | 1.230 | 1.247 | 0.029 |
| BH | Surface | 3.920 | 4.260 | 3.860 | 4.013 | 0.216 |
| GC234 | Surface | 4.290 | 4.930 | - | 4.610 | 0.453 |
| GC234 | Surface | 14.780 | 11.960 | 12.660 | 13.133 | 1.468 |
| GC234 | Surface | 1.290 | 1.290 | 1.220 | 1.267 | 0.040 |
| GC234 | Surface | 12.800 | 20.870 | 17.570 | 17.080 | 4.057 |
| GC234 | Surface | 1.550 | 1.570 | 1.450 | 1.523 | 0.064 |
| GC234 | Surface | 4.690 | 4.930 | 4.930 | 4.850 | 0.139 |

Sediment grain analysis was conducted on Cascadia Margin cores from sites C1, C7 and C9. With the exception of the surface depth of C1 all samples were well sorted silt and clay. The C1 surface sample contained 59.4% sand. Particle size phi 9 (1.95 μm) ranged from 20.77 to 45.41% for all of the samples that were analyzed. Vibration in the laboratory prohibited grain size analysis smaller the phi 9.

Table 3: Grain size analysis of cores from Cascadia Margin sites C1, C7 and C9. Data presented represent the percent of the sediment particles that fall in the range of phi size classes.

Sample Depth | phi

| (cm) | | 4 | 4.5 | 5 | 5.5 | 6 | 7 | 8 | 9 |
|------|---------|-----|-------|-------|-------|-------|-------|-------|-------|
| C9 | 5-10 | 100 | 94.72 | 88.38 | 81.71 | 75.01 | 61.32 | 48.17 | 36.83 |
| C9 | 15-20 | 100 | 97.27 | 93.24 | 86.63 | 81.20 | 66.05 | 51.87 | 35.84 |
| C9 | 35-40 | 100 | 95.61 | 92.52 | 93.99 | 86.05 | 74.43 | 59.83 | 45.01 |
| C9 | 45-50 | 100 | 97.49 | 92.47 | 84.52 | 76.84 | 67.28 | 41.26 | 30.05 |
| C9 | 75-85 | 100 | 99.84 | 98.42 | 92.78 | 88.18 | 69.97 | 52.64 | 35.76 |
| C9 | 105-120 | 100 | 99.57 | 97.46 | 90.00 | 81.45 | 63.82 | 47.01 | 32.75 |
| C9 | 145-155 | 100 | 96.80 | 93.78 | 88.63 | 81.95 | 67.12 | 51.27 | 39.49 |
| C9 | 295-300 | 100 | 90.19 | 87.46 | 60.91 | 73.84 | 59.41 | 51.99 | 34.81 |
| C9 | 300-310 | 100 | 91.32 | 88.97 | 80.82 | 74.21 | 61.11 | 51.46 | 37.20 |
| C1 | 0-10 | 100 | 94.66 | 92.06 | 92.25 | 87.12 | 78.59 | 63.18 | 45.41 |
| C1 | 20-30 | 100 | 96.64 | 92.46 | 84.78 | 58.10 | 49.80 | 40.03 | 24.71 |
| C1 | 30-40 | 100 | 94.84 | 90.37 | 84.18 | 78.44 | 61.12 | 44.65 | 29.41 |
| C1 | 40-50 | 100 | 98.63 | 94.15 | 85.70 | 78.86 | 64.47 | 46.60 | 30.72 |
| C7 | 200 | 100 | 98.01 | 94.98 | 90.83 | 83.79 | 65.79 | 49.06 | 31.09 |
| C7 | 270 | 100 | 95.66 | 90.58 | 82.81 | 76.79 | 60.68 | 45.19 | 30.77 |
| C7 | 280 | 100 | 98.67 | 93.84 | 86.29 | 76.91 | 58.50 | 41.35 | 26.03 |
| C7 | 300 | 100 | 93.90 | 86.53 | 76.88 | 68.37 | 51.55 | 35.87 | 20.77 |

b). Hydrate Gas Content

Hydrate content was analyzed on samples from GOM and compared to HMMV (Table 4). Samples from the HMMV contained 99.5% methane. The GOM hydrates ranged from 29.7 to 73.5% methane, 8.6 to 15.3% ethane, 11.6 to 36.6% propane, and 2.0 to 9.7% isobutane. Butane, pentane and hexane ranged from 0.1 to 3.2%. In the Gulf of Mexico yellow surface hydrates contained oil between the lattice. Comparison of hydrates with and without oil saturated lattice showed that there was not a difference in the gas content. However, there is a difference in the gas content between the two sample regions of Bush Hill and Green Canyon with samples at Bush Hill containing a higher percentage of methane and Green Canyon more ethane and isobutane. Further investigation is needed to determine the factors that control variation in the lattice content and saturation. Hexane was observed in one hydrate with a relatively low methane content and a high propane concentration. This suggests that this is hydrate structure H and is currently being confirmed with x-ray diffraction at the DOE Argonne National Laboratory. The HMMV hydrates have been confirmed to contain structure I, while the GOM is a mix structure I and II and possibly structure H.

Table 4: Hydrate content of samples taken from the Haakon Mosby Mud Volcano and the Texas-Louisiana Shelf. Stations named Bush Hill and Green Canyon are located in the GOM. Gases from methane (C1) to hexane (C6) were compared for the present composition.

| Sample ID | % Hydrocarbon composition | | | | | | |
|---------------------|---------------------------|----------------|----------------|--------------------------|----------------|----------------|-----|
| | C ₁ | C ₂ | C ₃ | <i>i</i> -C ₄ | C ₄ | C ₅ | |
| Haakon Mosby MV | 99.5 | 0.1 | 0.1 | 0.1 | 0.1 | 0.0 | 0.1 |
| Bush Hill White | 72.1 | 11.5 | 13.1 | 2.4 | 1.0 | 0.0 | 0.0 |
| Bush Hill Yellow | 73.5 | 11.5 | 11.6 | 2.0 | 1.0 | 0.1 | 0.2 |
| Green Canyon White | 66.5 | 8.9 | 15.8 | 7.2 | 1.4 | 0.1 | 0.1 |
| Green Canyon Yellow | 69.5 | 8.6 | 15.2 | 5.4 | 1.2 | 0.0 | 0.0 |
| Bush Hill | 29.7 | 15.3 | 36.6 | 9.7 | 4.0 | 3.2 | 1.6 |

c). $\delta^{13}\text{C}$ Hydrates

Stable carbon isotope analysis is employed to determine the relative contribution of biogenic and thermogenic source(s) to the gases in hydrates. Thermogenic methane is more isotopically enriched in C^{13} with an approximate range in values from -30 to -45 ‰. Biogenic methane is substantially depleted in C^{13} with values that typically range between -60 to -70 ‰ and have been measured to be more depleted in sites where the methane is recycled in the sediments. For this document $\delta^{13}\text{C}$ is compared from the HMMV, CM, and GOM. The hydrates from the GOM show a strong thermogenic isotope signature in the ethane to pentane gases (Figure 1). Pentane was isotopically enriched relative to the other gases with an average of -24.75 ± 1.67 for 8 hydrate samples. The gases with lower molecular weights had depleted isotope values with ethane $\delta^{13}\text{C}$ the lowest averaging -29.14 ± 0.62 ‰ for 18 hydrate samples. An interesting result of the analysis was the difference in the ranges of the GOM gases, where ethane to pentane variation was low, the methane variation was greater. Methane isotope ratios varied from -49.37 to -33.49 ‰ with an average and standard deviation of -45.45 ± 3.96 ‰. This result suggests a variation in the biogenic cycling of the methane between the 18 samples. This statement is supported with the large $\delta^{13}\text{C}$ variation in the CO_2 found in the hydrates. In 17 hydrate samples the values ranged from -16.77 to 18.83 ‰. The CO_2 is expected to become more enriched in C^{13} as it is reduced to methane by bacteria.

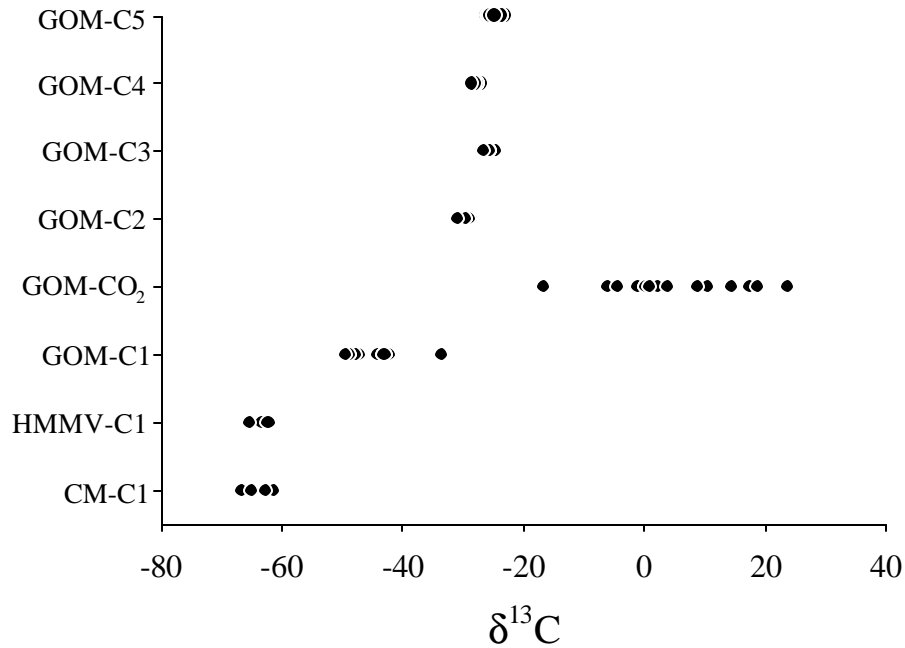


Figure 1: Stable carbon isotope analysis of hydrate gases. Samples are from the Gulf of Mexico (GOM), Haakon-Mosby Mud Volcano (HMMV) and the Cascadia Margin (CM). Gases analyzed include methane to pentane (C1 to C5) and CO₂.

The HMMV and CM hydrates contained only methane (Table 4). The methane $\delta^{13}\text{C}$ ranged from -65.36 to -62.14‰ in 6 hydrates from the HMMV and -66.64 to -61.27‰ for six samples from the Cascadia Margin (Figure 1). These results coupled with the analysis of the hydrate content indicate that methane in hydrates at these sites is formed biogenically.

d). $\delta^{13}\text{C}$ Organic Sediments

Analysis of the sediment carbon sources was conducted to advance understanding of the methane hydrate content and lattice saturation. The $\delta^{13}\text{C}$ analysis of the sediments provides information on the primary sources of carbon in the sediment. Stable carbon isotope values in the range of -18 to -22‰ in these study sites represent carbon from ocean water column primary production. The methane cycling into the sediment organic carbon has a complex series of cycles that can influence these isotope signatures. More C^{13} depleted values, ranging from -30 to -40‰ indicates thermogenic methane. Biogenic methane has potential to result in isotope signatures, more depleted, in the range of the methane measured in CM and HMMV hydrates. Another cycle that can contribute to the C^{13} depleted signatures is the oxidation of methane and fixation of CO₂ (chemosynthesis). Additional tracers are needed to determine the sources of carbon in these sediments. The current stable carbon isotope data suggests that there is a large variation in the carbon cycles in the hydrate regions. Figure 2 presents $\delta^{13}\text{C}$ for organic sediments from HMMV,

CM and GOM. The control value is from the GOM, outside regions with hydrates. This value at -21.50‰ represents a strong water column phytoplankton production input (Figure 2). At many of the sites that were surveyed the $\delta^{13}\text{C}$ are substantially lower than the control site. The most depleted $\delta^{13}\text{C}$ signatures are observed in the HMMV and GOM-BP. The isotope ratios at the individual sites are variable suggesting that there is a large range in the methane cycling and the contribution to organic matter in the sediments. Future work will apply additional tracers to understand this variation and the influence on hydrate formation, stability and lattice saturation.

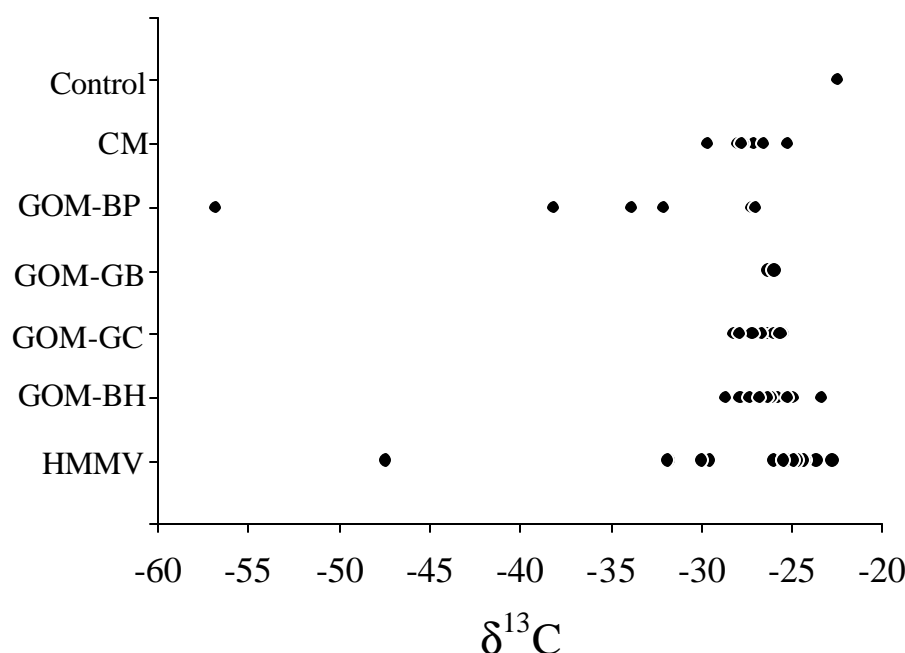


Figure 2: Stable carbon isotope analysis of organic carbon in shallow sediments through regions surrounding active methane hydrate beds. Samples were taken in the Gulf of Mexico (GOM), Cascadia Margin (CM), and Haakon-Mosby Mud Volcano (HMMV). Different sites sampled in the Gulf of Mexico include a brine pool (BP), Garden Bank (GB), Bush Hill (BH), and Green Canyon (GC).

Vertical $\delta^{13}\text{C}$ profiles of organic carbon in the sediments were analyzed in hydrate beds on the Cascadia Margin (Figure 3). Cores 1, 6, and 7 were taken in an active hydrate region while core 9 was taken outside of the active hydrate bed. The segments of core 7 that are presented were in regions where hydrates were found. There was a wide range in $\delta^{13}\text{C}$ values between the sites and through the cores, with $\delta^{13}\text{C}$ values between -29.68 and -18.67 . The sub-samples from core 7 were observed to have the most depleted C^{13} . Core 6 was found to have the most enriched C^{13} values, indicating ocean phytoplankton was a significant carbon source. As noted between different sites and ocean regions, the large range in values through the vertical profiles indicates that there was a large variation in methane contribution to the sediment carbon cycle. Future work will employ carbon isotope analysis of DIC and bacterial biomarkers (hopanes) to assess the variation in the sediment organic carbon isotope analysis.

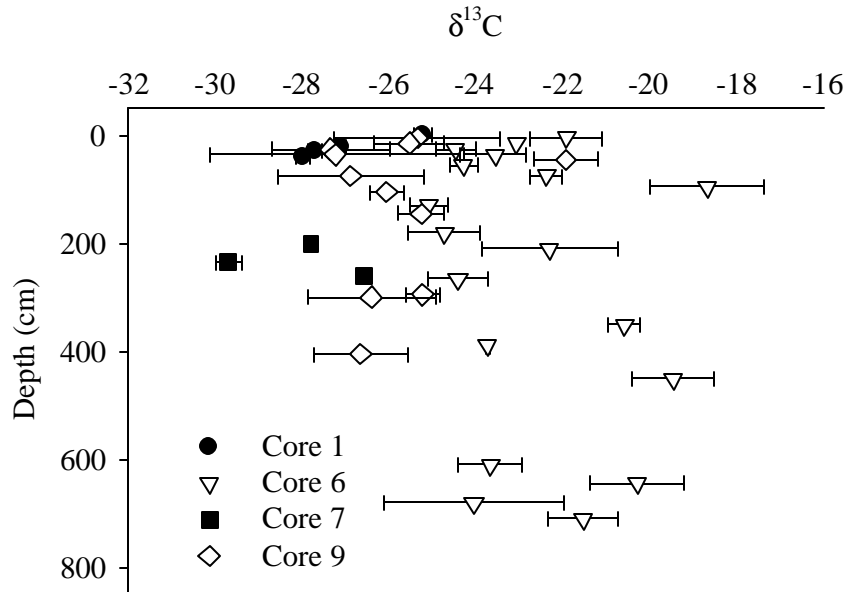


Figure 3: Stable carbon isotope analysis of sediment organic carbon on samples from the Cascadia Margin.

e). $\delta^{13}\text{C}$ Carbonates

Stable carbon isotope analysis of carbonates has been initiated. The existing data shows an interesting trend in the $\delta^{13}\text{C}$ through the vertical profile, with values ranging between 2.82 and -14.77‰ (Table 5). The C^{13} enriched values, 2.82 to -2.47‰ indicate the carbonate is a biogenic source. At 130-140 cm into the core the C^{13} depleted value of -14.77‰ suggests the formation of carbonate is partially from authigenic cycles. Authigenic carbonate has been measured to be C^{13} depleted at approximately -60‰ on the Blake Ridge. Completion of this data will assist in analysis of the amount of methane this is oxidized through the water column.

Table 5: Preliminary analysis of sediment bicarbonate $\delta^{13}\text{C}$ in Core 6 from the Cascadia Margin.

| Sample | Depth (cm) | $\delta^{13}\text{C}$ | $\delta^{13}\text{C}$ | $\delta^{13}\text{C}$ | Average | s.d. |
|--------|------------|-----------------------|-----------------------|-----------------------|---------|------|
| Core 6 | 25-30 | 3.49 | 3.15 | 1.82 | 2.82 | 0.88 |
| Core 6 | 130-140 | -13.97 | -14.62 | -15.71 | -14.77 | 0.88 |
| Core 6 | 390-400 | -6.14 | -5.52 | n.d. | -5.83 | 0.44 |
| Core 6 | 450-460 | -0.39 | -1.9 | n.d. | -1.15 | 1.07 |
| Core 6 | 645-655 | -4.81 | -4.89 | -4.79 | -4.83 | 0.05 |
| Core 6 | 680-690 | -2.47 | n.d. | n.d. | -2.47 | - |

f). $\Delta^{14}\text{C}$ Methane Hydrates

$\Delta^{14}\text{C}$ and $\delta^{13}\text{C}$ of the methane in hydrates was measured to assist in understanding the methane sources (Figure 4). The $\delta^{13}\text{C}$ of the methane from GOM was enriched in ^{13}C showing the source was thermogenic. Cascadia Margin methane $\delta^{13}\text{C}$ was isotopically lighter showing a biogenic source. The $\Delta^{14}\text{C}$ of methane in both sites was depleted suggesting an old (thermogenic carbon source). For the Cascadia Margin the combination of biogenic $\delta^{13}\text{C}$ values and aged $\Delta^{14}\text{C}$ suggests a strong vertical migration of the methane. This will be confirmed in subsequent analysis of the organic sediment $\Delta^{14}\text{C}$ compared with the methane.

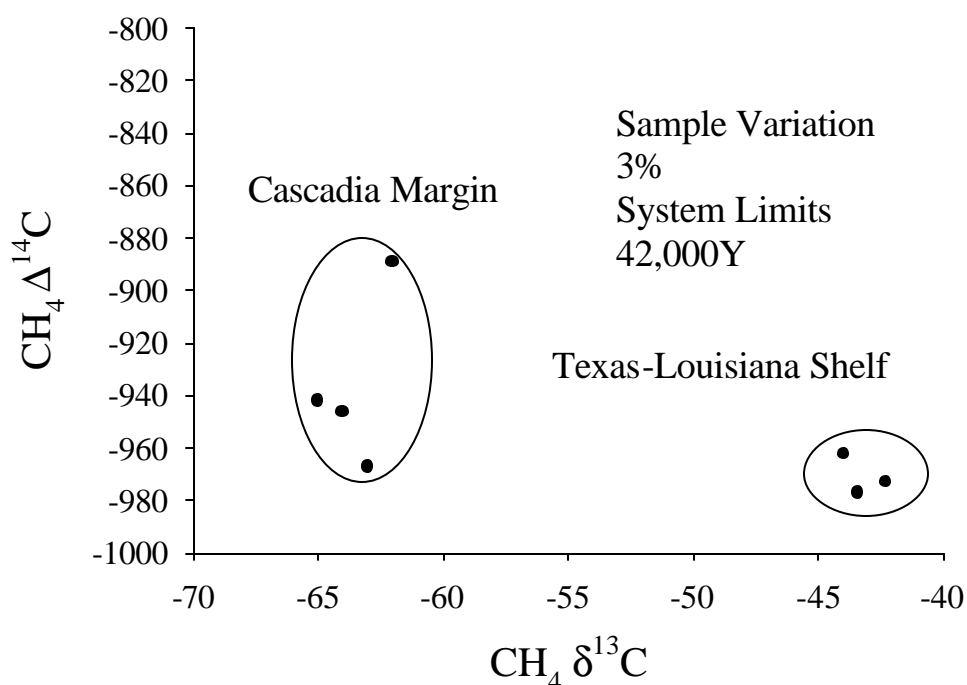


Figure 4: Stable and radiocarbon isotope analysis of methane in hydrates from the Cascadia Margin and Texas-Louisiana Shelf.

g). $\Delta^{14}\text{C}$ Organic Sediments

Four sites were compared for the $\Delta^{14}\text{C}$ of organic carbon in sediments where methane hydrates were present. The range in percent modern carbon (PMC) between the sites was approximately 10-100 PMC (Figure 5). Bush Hill was found to have the most depleted $\Delta^{14}\text{C}$ with values ranging from 10-20 PMC. These values are likely due to a combination of thermogenic methane and petroleum seeping in this region.

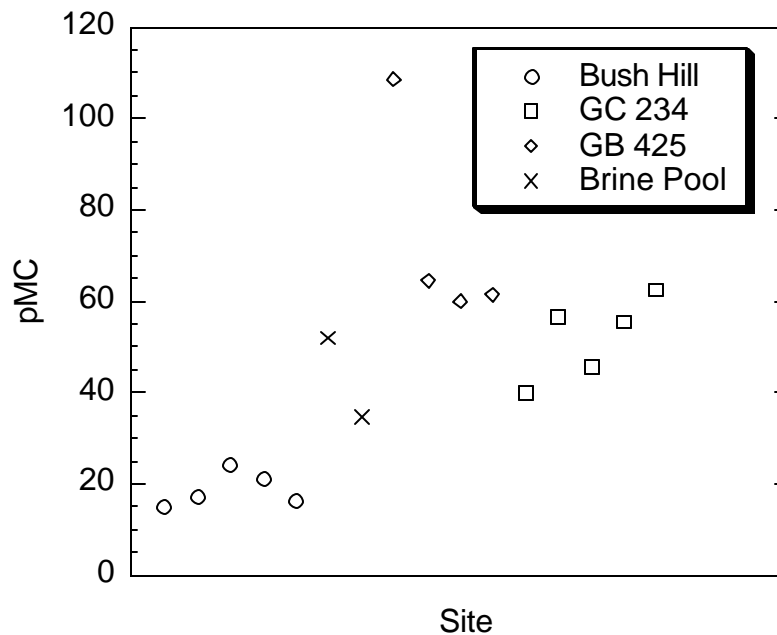


Figure 5: Radiocarbon isotope analysis of organic sediments in the Gulf of Mexico along the Texas-Louisiana Shelf.

6. Summary

- a). The percent organic carbon in CM sediments was low. Values ranged from 0.340 to 0.738%. In comparison the GOM samples ranged from 1.25 to 17.08%. The high carbon content in this system results from petroleum seepage.
- b). The sediments consisted of well sorted silt and clay. Particle size analysis of cores from the CM found that between 20.77 to 45.41% of the grains were 1.95 μm or smaller.
- c). The methane content in hydrates from the Gulf of Mexico varied between 73.5 and 29.7%. There was a large concentration of propane in the GOM hydrates indicating thermogenic origin of the gases.
- d). Stable carbon isotope analysis of hydrate methane on HMMV and CM samples shows that the source is biogenic. The isotope analysis of the gases from the GOM samples indicates a thermogenic origin and biogenic cycling of the methane.
- e). Stable carbon isotope analysis of the organic matter in sediments from GOM, CM and HMMV show a high variation in values. Carbon sources for this organic matter include marine phytoplankton, biogenic methane and thermogenic methane. In many of the samples methane is a large fraction of the sediment carbon cycling.

f). Preliminary stable carbon isotope analysis of the carbonate in sediments suggests that the source is dominantly biogenic. In one sample a more C^{13} depleted signature indicates authigenic input.

g). Radio carbon isotopes in the methane from hydrates was depleted in ^{14}C for samples from the GOM and CM. This confirms that the methane in the GOM is thermogenic. The depleted ^{14}C relative to the biogenic stable carbon isotope ratio in the methane from the Cascadia Margin suggests there is a vertical migration of the methane. The $\Delta^{14}C$ of the organic carbon in the sediments from the GOM was large in the range of values. Depleted values of samples from Bush Hill suggests that thermogenic methane is a large contribution to the carbon cycle at this site.

7. Literature Cited

Bauer, J. E., E. R. M. Druffel, P. M. Williams, D. Wolgast, and S. Griffin. 1998. Time dependent variations in the natural radiocarbon content of dissolved organic matter in the eastern north Pacific Ocean. *J. Geophys. Res.* **103**, 2867-2882.

Bauer, J. E., P. M. Williams, and E. R. M. Druffel. 1992. ^{14}C activity of dissolved organic carbon fractions in the central North Pacific and Sargasso Sea. *Nature* **357**, 667-670.

Borowski, W.S., C.K. Paull, W. Ussler III. 1996. Marine pore-water sulfate profiles indicate in situ methane flux from underlying gas hydrate. *Geology* **24**, 655-658.

Borowski, W.S., C.K. Paull, W. Ussler III. 1997. Carbon cycling within the upper methanogenic zone of continental rise sediments: An example from the methane-rich sediments overlying the Blake Ridge gas hydrate deposits. *Mar. Chem.* **57**, 299-311.

Cherrier, J., J. E. Bauer, E. R. M. Druffel, R. B. Coffin, J. P. Chanton. 1999. Radiocarbon in Marine Bacteria: Evidence for the Age of Assimilated Organic Matter. *Limnology and Oceanography* **44**(3), 730-736.

Estep, M.L., F.R. Tabita, P.L. Parker, and C. Van Baalen. 1978. Carbon isotope fractionation by ribulose 1,5-bisphosphate carboxylase from various organisms. *Plant Physiol* **61**, 680-687.

Fogel, M.L. and L.A. Cifuentes. 1993. Isotopic fractionation during photosynthesis: Interpretation for the fossil record. In *Organic Geochemistry*, Eds. M. Engel and S. A. Macko - Eds.

Galehouse, J. S. 1971. Sedimentation analysis. In *Procedures in Sedimentary Petrology* (ed. R. Carver) John Wiley pp. 69-94.

- Gearing, P., F.E. Plucker, and P.L. Parker. 1977. Organic carbon stable isotope ratios of continental margin sediments. *Mar. Chem.* **5**, 251-266.
- Ingram, R. 1971. Sieve Analysis. In *Procedures in Sedimentary Petrology* (ed. R. Carver) John Wiley pp. 49-67.
- Parsons, T.R., Y. Maita, and C.M. Lalli. 1984. A manual of chemical and biological methods of seawater analysis. Pergamon Press, New York.
- Rau, G.H., T. Takahashi, and D.J. Des Marais. 1989. Latitudinal variation in plankton $\delta^{13}\text{C}$: implication for CO_2 and productivity in past oceans. *Nature* **341**, 516-518.
- Sackett, W.M. 1991. A history of the $\delta^{13}\text{C}$ composition of oceanic plankton. *Mar. Chem.* **34**, 153-156.
- Von Reden, K.F., A.P. McNichol, J.C. Peden, K.L. Elder, A.R. Gagnon, R.J. Schneider. 1997. AMS measurements of the ^{14}C distribution in the Pacific Ocean. *Nucl. Instr. and Meth. B* **123**, 438-442.
- Whelan, T., M.W. Sackett, and C.R. Benedict. 1973. Enzymatic fractionation of carbon isotopes by phosphoenolpyruvate carboxylase from C_4 plants. *Plant Physiol.* **51**, 1051-1054.
- Williams, P. M. and E. R. M. Druffel. 1987. Radiocarbon in dissolved organic matter in the central North Pacific Ocean. *Nature* **330**, 246-248.

High-field NMR Analyses of Structure I Methane Hydrate

James P. Yesinowski, Code 6120, Naval Research Laboratory

We have carried out a variety of proton and carbon NMR experiments on well-characterized synthetic Structure I methane hydrate produced and provided by the group of Laura Stern and Steve Kirby at the USGS Menlo Park. The samples were produced from melting powdered ice in the actual NMR sample containers under a high methane pressure [L.A. Stern et al., 1996]; they were shipped to NRL and stored in liquid nitrogen.

Experimental

Wide-line proton NMR experiments were carried out on two spectrometers, a Bruker DMX-300 operating at 7.05T and a Bruker DMX-500 operating at 11.7 T. Low-background high-power static proton probes with 5mm horizontal solenoidal coils were used. Samples were packed in short 5mm glass NMR tubes maintained at probe temperatures in the vicinity of 173K by a flow of nitrogen gas cooled in a liquid nitrogen heat exchanger and temperature-regulated by a heater in the glass dewar inside the probe.

^{13}C cross-polarization magic-angle-spinning (CP-MAS) NMR spectra were obtained on a Bruker DMX-500 operating at 11.7 T. The sample was synthesized from powdered ice packed into a 7mm o.d. zirconia rotor with a zirconia cap. It was shipped from USGS to NRL in a liquid nitrogen storage dewar, and maintained at liquid nitrogen temperatures except during its transfer to the NMR probe. A 7mm broadband Bruker CP-MAS probe with a pneumatic insertion tube for the rotor was used. Variable-temperature operation down to a nominal 163K was achieved by nitrogen gas flowing through two liquid nitrogen heat exchangers in series and temperature-regulated by a heater in the probe in the bearing gas line for the stator. The instrument manufacturer initially asserted that it would be possible to load a precooled sample into a precooled probe around 173K. However, repeated attempts to do so over a long period of time led to rotors failing to insert into the coil region, and often jamming upon attempts to eject. Attempted solutions included enclosing the upper portion of the pneumatic stack in a plastic bag continually flushed with dry nitrogen, to prevent any possibility of frost condensation in the probe. Despite this and other efforts, it proved impossible to reliably insert rotors into the coil, much less to achieve sample spinning. A visit to NRL from a Bruker solids applications chemist confirmed the problem to Bruker, but they were unable to offer any solution. Indications are that slight dimensional changes affecting the curved trajectory path of the rotor into the coil region may be responsible. In general, 213K was about the lowest temperature at which other test samples could be successfully inserted and spun, although test samples starting at room temperature could be cooled down to 163K while spinning (at a reduced spin rate). On one occasion, during

an exploratory attempt to carry out a new type of non-spinning experiment, it was observed that the hydrate sample began spinning, albeit very slowly (500-800Hz) and rather unstably. The CP-MAS results presented here are from that occasion (the spinning rate was sufficient to narrow and resolve the peaks from the large and small cages).

Results

Proton NMR

The 300 MHz proton NMR spectrum of structure I methane hydrate at a nominal temperature of 163K is shown in Fig. 1. The top spectrum was obtained by Fourier-transforming the free induction decay acquired after a short delay of 4.5 μ s after a 90° pulse of 2.5 μ s. The proton NMR spectrum of a sample of methane hydrate prepared from D₂O has been reported [Davidson et al. 1977]; the narrow and constant width of the methane signal from 2-200K indicates that the methane molecules are rapidly tumbling at all temperatures, hence averaging out proton-proton dipolar interactions. The top spectrum in Fig. 1 shows three features: a very sharp peak on top, a somewhat broader peak of about 15 kHz half-height width, and a broader base extending over 100 kHz. Based upon the strength of the dipolar interactions and the results from Davidson et al., we can attribute the broadest signal to the water protons of the lattice, and the intermediate width signal to the methane protons of the clathrate. Because the dipolar interactions in this spin system are homogeneous in character, the NMR signals from these two components cannot be regarded as separate entities. For example, they exhibit identical spin-lattice relaxation behavior (see below).

The sharp peak in the spectrum of Fig. 1 (top) was unexpected. It was possible to irradiate the sample with a low power (1 kHz rf) continuous wave pulse placed 20 kHz off-resonance for a duration of 30 s, thereby saturating the NMR signal of the hydrate component. The resulting spectrum, shown as the bottom plot of Fig. 1, reveals that the sharp component does not arise from any species having a dipolar coupling with the methane hydrate protons (otherwise it would be saturated as well). In addition, the sharp component can be observed using a Carr-Purcell-Meiboom-Gill (CPMG) pulse sequence, as shown in Fig. 2. Based on this behavior, we assign the sharp peak to a small amount of “pore space methane” present in the sample as a result of the synthesis procedure. Presumably the ice or hydrate crystals can sinter and completely enclose methane gas at high pressure. The chemical shift of 0.0 ppm (referenced to liquid acetone at low temperature) is reasonable for methane gas/liquid, and the linewidth of 750 Hz may be due to magnetic susceptibility broadening or a distribution of environments. That the former is the case is suggested by a ¹H MAS-NMR spectrum obtained on the DMX-500 during the course of the CP-MAS experiment discussed below: the linewidth was reduced to 0.1 ppm (50 Hz), and the peak position was 1.9 ppm to lower frequency from that of adamantane.

This ability to observe trapped methane by proton NMR is significant, both for the characterization of synthetic samples and the possibility that trapped methane gas may be present in natural samples. Observation by NMR of its unanticipated presence has led the USGS group to slightly modify their sample preparation procedure to minimize or eliminate its presence.

The proton spin-lattice relaxation time T_1 was determined using a saturation recovery pulse sequence. The data points at 300 MHz are plotted in Fig. 3, along with a single-exponential theoretical recovery curve for a T_1 value of 6.76 s. The agreement is very good. The T_1 value measured at 500 MHz and a similar temperature is very close to this value, indicating that the relaxation is due to motions in the “extreme-narrowing limit”, i.e. faster than ca. 10^{-9} s. Dipolar interactions modulated by the nearly unrestricted rotation of the methane molecules is a likely candidate for the relaxation mechanism, although further work is needed to establish this point. If so, one might expect that the T_1 value at a given temperature would reflect the hydration number of the hydrate (and certainly the structural type).

Carbon NMR

The ^{13}C CP-MAS NMR spectrum of methane hydrate at a nominal temperature of 193K is shown in Fig. 4 (an expansion of part of the entire spectrum). The spinning rate varied between 812 and 620 Hz), and the cross-polarization contact time was 15 ms. The chemical shift referencing was carried out by using a separate rotor containing adamantane as a secondary chemical shift reference. A significant temperature dependence of the high-frequency peak of adamantane was noted, so it was assumed that the low-frequency peak represented a more satisfactory reference. The chemical shifts of the peaks assigned to methane molecules in the large and small cages are -6.62 ppm and -4.21 ppm respectively. These values are about 1.4 ppm to lower frequency of the corresponding values previously reported [Ripmeester and Ratcliffe 1988], although the latter values may have been referenced in a less satisfactory way. The *difference* between the two chemical shift values, 2.41 ppm, agrees very closely with the previously reported value of 2.37 ppm. The half-height linewidths of the large and small cage peaks are 0.36 ppm and 0.44 ppm respectively, and these small values suggest a well-ordered crystalline environment.

The ratio of the large to small cage peak integrals was measured to be 3.39. If we make the reasonable assumption that the 15 ms CP contact time yields signal intensities proportional to the cage occupancies, then we can calculate a fractional occupancy ratio of small/large cages of 0.885. This can be compared to the corresponding ratio of 0.916 determined previously [Ripmeester and Ratcliffe 1988] for a methane hydrate prepared from ice at -40°C . The statistical thermodynamic analysis approach adopted there, along with measured chemical potentials from xenon hydrates, yielded *absolute* occupancies for large and small cages of 0.97 and 0.89 respectively, and a hydration number of 6.05. Given the slightly different preparation conditions and the experimental errors involved, the present results can be considered to be in good agreement, and likely to yield very similar values for absolute occupancies and hydration number.

Conclusions

The proton NMR spectra of Structure I methane hydrates at low temperatures can identify the presence of trapped methane gas/liquid that is not part of the hydrate structure. The spin-lattice relaxation time T_1 is reasonably short, field-independent, and likely to reflect the amount of clathrate methane present relative to the water component (and thus the hydration number), although this remains to be proven.

The ^{13}C CP-MAS spectrum obtained yields accurate values for the chemical shifts and relative cage occupancies of methane in the large and small cages. However, the present design of the (new generation) Bruker MAS-NMR probe is not suitable for routine analyses of samples retrieved from the ocean at the low temperatures necessary to stabilize the Structure I hydrates. Maintaining samples at a higher temperature and pressure is not feasible in the present probe. A redesigned probe or probe modification may be more suitable. Also, attention should be given to the development of alternative *non-spinning* techniques for the analysis of cage occupancies in hydrate samples. This is true because of the general difficulties that are encountered in the packing of samples and spinning at low temperatures.

References

D.W. Davidson, S.K. Garg, S.R. Gough, R.E. Hawkins and J.A. Ripmeester, *Can. J. Chem.*, **55**, 3641 (1977).

L.A. Stern, S.H. Kirby, W.B. Durham, *Science*, **273**, 1843 (1996).

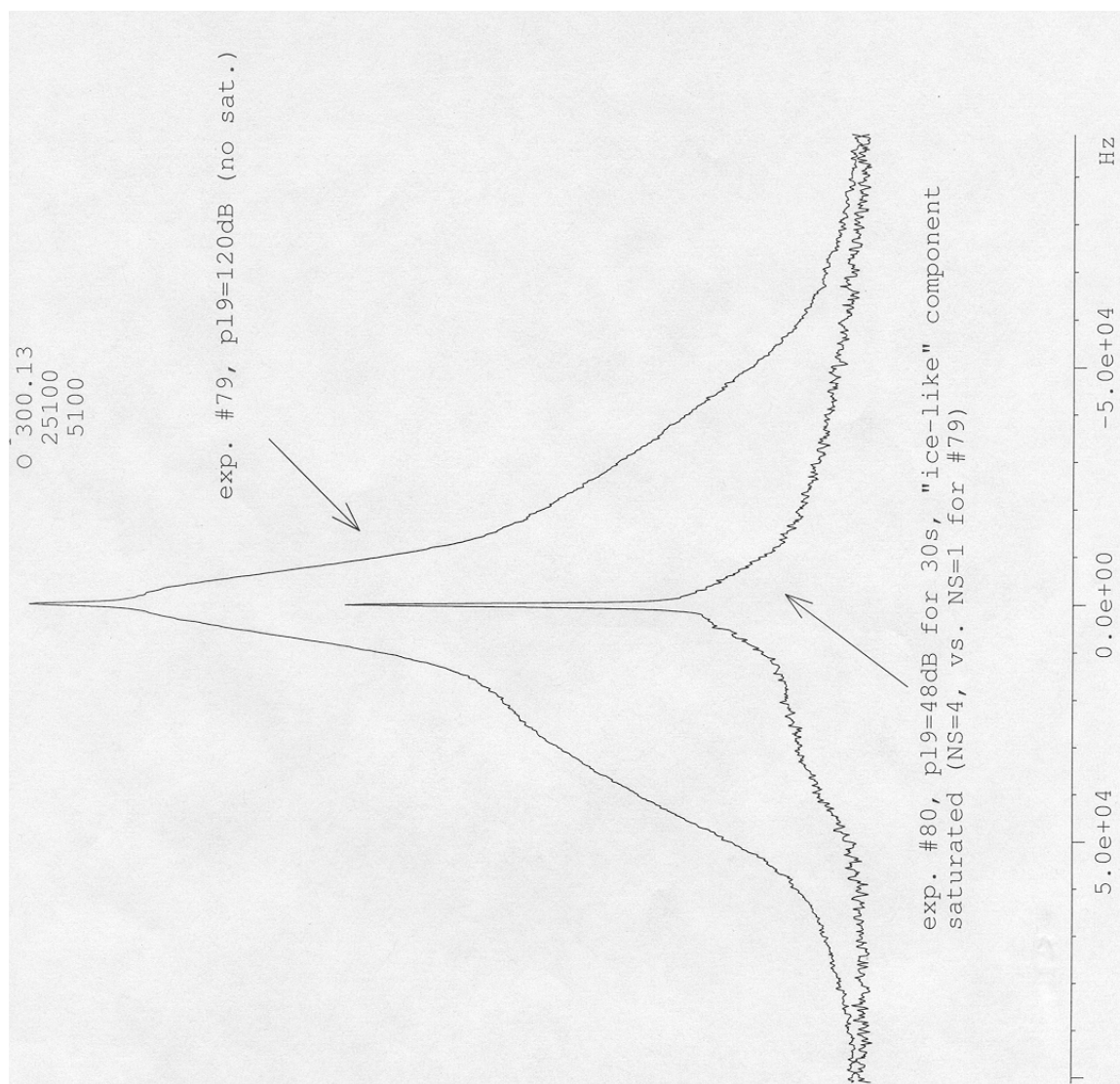


FIGURE 1: Proton NMR Spectra of Structure I Methane Hydrate (see text for details)

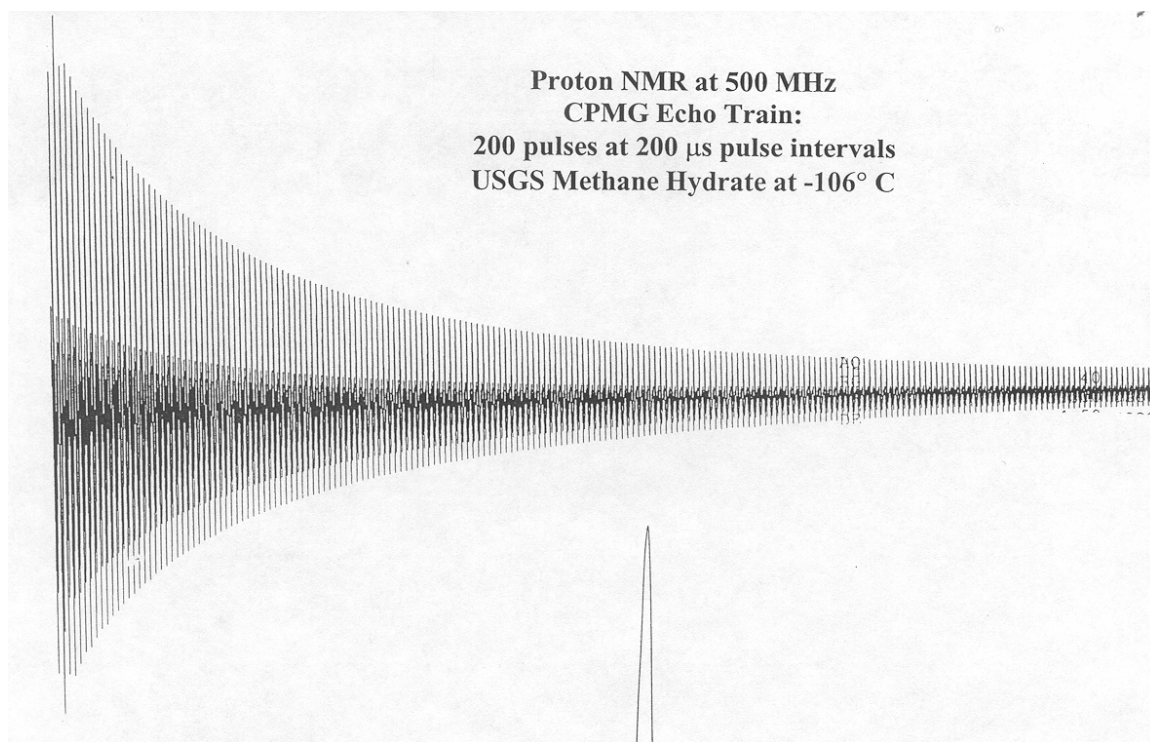


FIGURE 2: CPMG Pulse Sequence, Showing Slow Decay of Proton NMR Signal Arising From Pore Space Methane

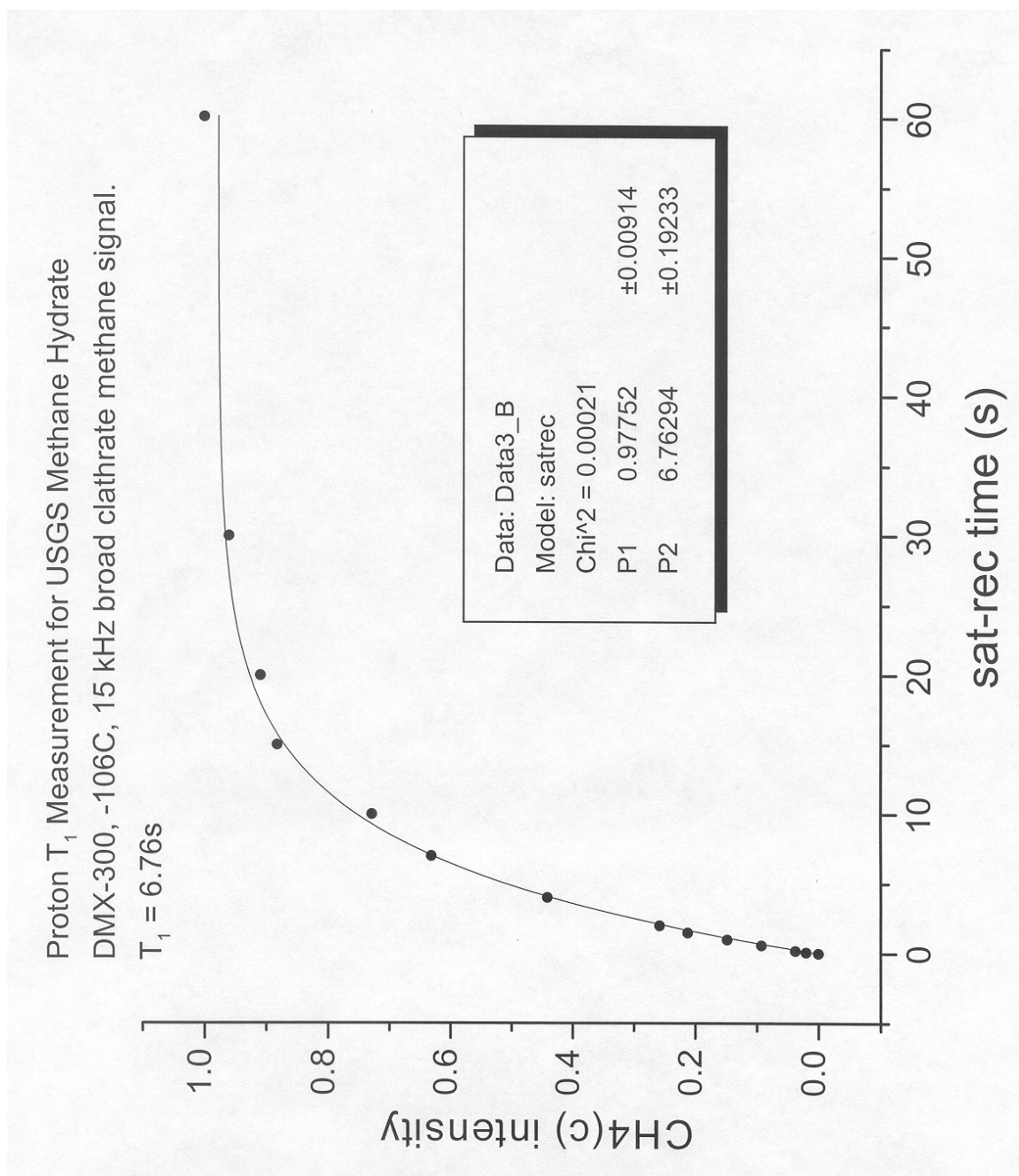


FIGURE 3: Proton NMR T_1 Spin-Lattice Relaxation Time Measurement

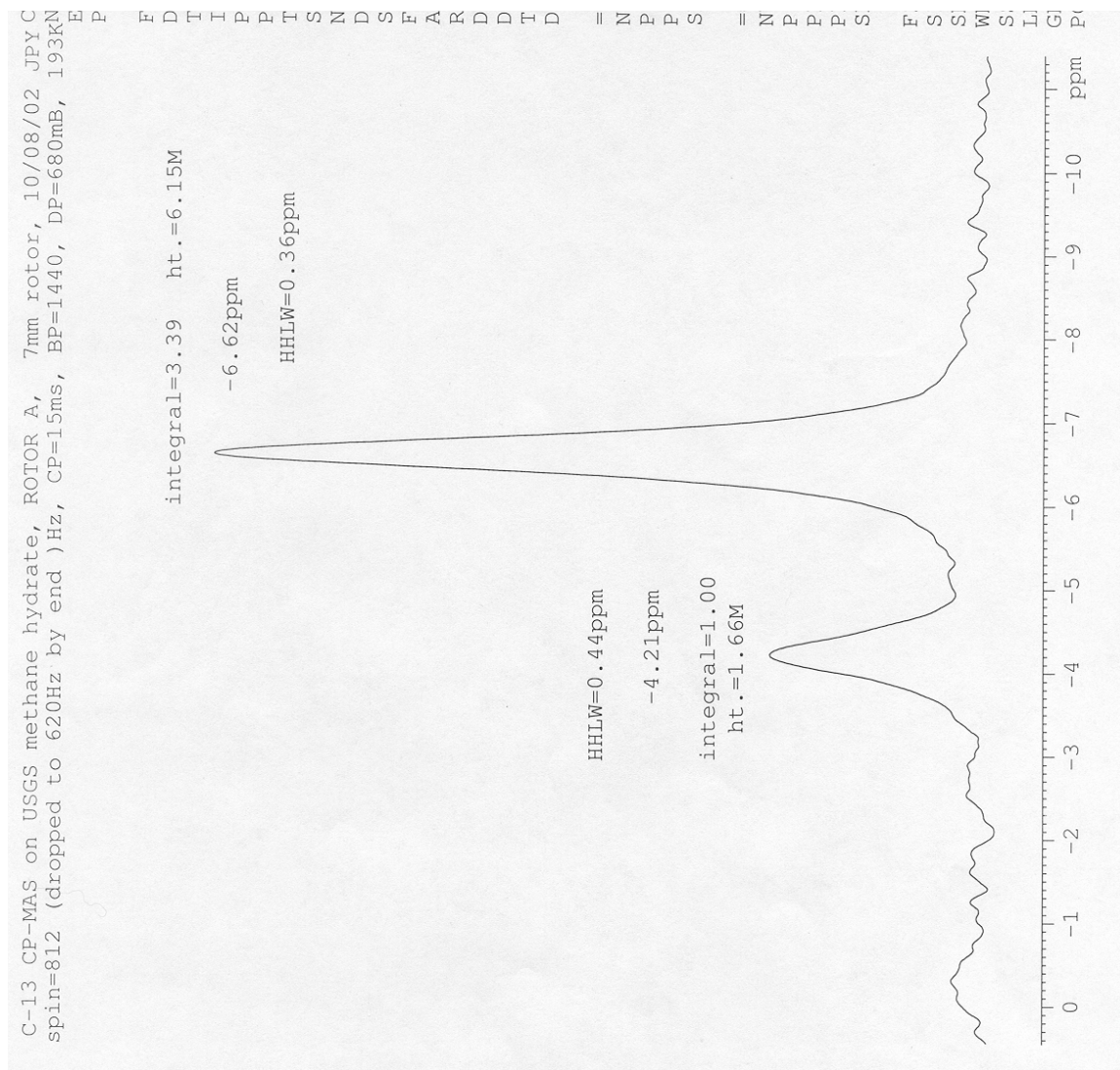


FIGURE 4: ^{13}C CP-MAS NMR Spectrum of Methane Hydrate, Resolving Methane in Small and Large Cages